DETECTION OF CARBENDAZIM RESIDUES WITH A COLORIMETRIC SENSOR BASED ON GOLD NANOPARTICLES

Y. Ma [1,2], H. Jiang [1], C. Shen [3], Ch. Hou [1*], D. Huo [1*], H. Wu [1], M. Yang [1]

[1] College of Bioengineering, Chongqing University,
Chongqing 400044, China; e-mail: huodq@cqu.edu.cn; houcj@cqu.edu.cn
[2] College of Bioengineering, Sichuan University of Science and Engineering,
Zigong, 643000, P.R.China
[3] National Engineering Research Center of Solid-State Brewing,
LuzhouLaojiao Group Co.Ltd., Luzhou, Sichuan 646000, China

Carbendazim is among the most popular benzimidazole bactericides that are widely used to boost food production, and its residue poses a great threat to human health and the environment. In this paper, we presented a colorimetric sensor based on gold nanoparticles (Au-NPs) for the detection of carbendazim residues. The Au-NPs were stabilized by citric acid synthesized by chloroauric acid and sodium citrate with a diameter of about 13 nm. Upon reaction with carbendazim, the sensor gave a clear color change that could be distinguished with the naked eye. Thus we elaborated a new method for rapid determination of this benzimidazole bactericide. After optimization of the detection conditions, the sensor showed a very good linear relationship with the carbendazim concentrations varying from 10 to 600 ppb with a detection limit down to 3.4 ppb (S/N=3). These preliminary results demonstrate that the presented sensor is promising for fast carbendazim analysis.

Keywords: *gold nanoparticles, carbendazim, colorimetric sensor, detection.*

ОПРЕДЕЛЕНИЕ ОСТАТКОВ КАРБЕНДАЗИМА С ПОМОЩЬЮ КОЛОРИМЕТРИЧЕСКОГО СЕНСОРА НА ОСНОВЕ НАНОЧАСТИЦ ЗОЛОТА

Y. Ma [1,2], H. Jiang [1], C. Shen [3], Ch. Hou [1*], D. Huo [1*], H. Wu [1], M. Yang [1]

УДК 620.3;543.432

[1] Колледж биоинженерии, Университет Чунцина,
Чунцин, 400044, Китай; e-mail: huodq@cqu.edu.cn; Houcj@cqu.edu.cn
[2] Колледж биоинженерии, Сычуаньский технический университет, Цигун, 643000, Китай
[3] Национальный научно-исследовательский центр полупроводникового пивоварения,
LuzhouLaojiao Group Co.Ltd., Лучжоу, Сычуань, 646000, Китай

(Поступила 16 декабря 2015)

Представлен колориметрический сенсор на основе наночастиц золота (Аи-НЧ) для обнаружения остатка карбендазима – одного из самых популярных бензимидазольных бактерицидов, которые широко используются при производстве пищевых продуктов. Его остаток представляет большую угрозу для здоровья человека и окружающей среды. Стабилизированные лимонной кислотой Аи-НЧ диаметром ~13 нм синтезированы с помощью хлорауриновой кислоты и цитрата натрия. При взаимодействии с карбендазимом сенсор показывает четкое изменение цвета, видимое невооруженным глазом, и демонстрирует значительные изменения при облучении УФ и видимым излучением, что свидетельствует о возможности его использования для быстрого определения карбендазима. После оптимизации условий обнаружения сенсор дает возможность определения концентраций карбендазима от 10 до 600 нг/г с низким пределом обнаружения до 3.4 нг/г (S/N = 3) и представляет значительный интерес для эспресс-анализа карбендазимов.

Ключевые слова: *наночастицы золота, карбендазим, колориметрический сенсор, детектирование.*

Introduction. Carbendazim, a benzimidazole, is among the most popular bactericides widely used in food production [1–3]. However, its residues pose a great potential threat to human health and the environment [4–6]. Therefore, the determination of carbendazim residues is of great importance in food safety and environment preservation.

Many traditional discrimination systems are reported for carbendazim residue analysis, for example, gas chromatography (GC) [7], liquid chromatography-mass spectrometry (LC-MS) [5, 8–11], high performance liquid chromatography (HPLC) [12–16], and capillary electrophoresis with mass spectrometry detection (CE-MS) [17]. However, in spite of the high precision, they are time-consuming and complicated. Recently several electrochemical sensors were developed to discriminate carbendazim and other pesticides [3, 4, 18–21]. Although the electrochemical method is simple and cost-effective, it is sometimes deficient in selectivity or stability. Thus, the development of a simple, rapid, and cost-effective sensor system for the detection of carbendazim is still urgently needed.

Gold nanoparticles (Au-NPs), one of the most commonly used nanomaterials, are employed as sensing materials for the detection of trace substances due to their excellent photoelectric properties [22–26]. Liu et al. [27] developed a highly sensitive and selective colorimetric sensor based on Au-NPs for cartap analysis with a detection limit of 0.04 mg/kg. Imene et al. [24] also used 4-amino-3-mercaptobenzoic acid functionalized gold nanoparticles to detect cyhalothrin through colorimetry. Some research groups investigated the possibility of carbendazim trace analysis on the basis of Au-NPs [28, 29]. For example, Strickland et al. [28] utilized cyclodextrin inclusion complexes on gold nano-rods to detect carbendazim through surface-enhanced Raman scattering. But the Raman spectrometer used to this end was a large and complex instrument. Thus, in our opinion, no study has been reported on detecting carbendazim via colorimetry based on Au-NPs.

Herein, we present a simple and effective colorimetric sensor for the discrimination of carbendazim on the basis of Au-NPs. It should be noted that electron-rich nitrogen exhibits a much stronger binding ability/affinity to Au-NPs [27]. Carbendazim contains several nitrogen atoms (–NH–/–N=) that can absorb onto the surface of Au-NPs. All the nitrogen atoms of carbendazim are bonded onto the surface of Au-NPs in acidic and alkaline environments. The aromatic structure in carbendazim improves the interaction between Au-NPs and carbendazim through the π-system [30]. Here we presented a carbendazim analysis in the neutral condition. As can be seen in SM. 1, upon addition of carbendazim, it was bonded onto the Au-NPs, which resulted in the electrostatic repulsion between the broken Au-NPs and the Au-NPs tending to assemble. The Au-NPs colloid color was changed from red to blue. This could be observed with the naked eye and was quantitatively monitored by a UV-vis spectrophotometer. The preliminary results demonstrate that the prepared Au-NPs sensor is promising for fast carbendazim analysis.

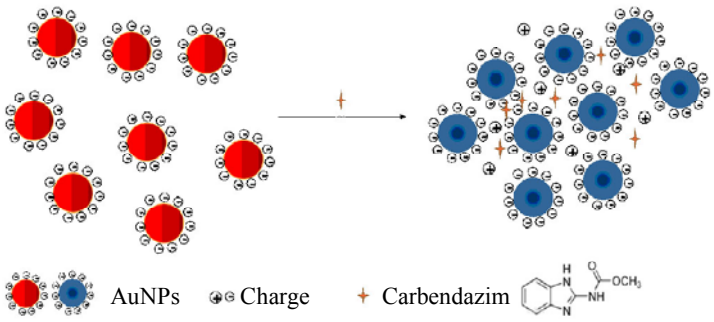

Experiment. *Chemicals and regents.* Chloroauric acid ($HAuCl_4 \cdot 4H_2O$) and sodium citrate ($C_6H_5Na_3O_7 \cdot 2H_2O$) were purchased from the National Pharmaceutical Group Chemical Reagent Co., Ltd. Carbendazim, trichlorfon, lindane, aminotriazole, trietazin, deltamethrin, triazolone, chlorpyrifos, and marathion were obtained from the Chongqing Entry Exit Inspection and Quarantine Bureau. All these chemicals were of analytical grade without further purification. Cabbages and apples were purchased from the local Wal–Mart supermarket. Tri-distilled water used here was generated by a Millipore Direct-Q Water system (Molsheim, France).

Synthesis of Au-NPs. Au-NPs were synthesized via reduction of $HAuCl_4 \cdot 4H_2O$ by $Na_3C_6H_5O_7 \cdot 2H_2O$ [31, 32]. Briefly, 1 mL of $HAuCl_4 \cdot 4H_2O$ solution (1 g/100 mL) was added to 100 mL of tri-distilled water, and the mixture was heated to reflux. Then 6 mL of $Na_3C_6H_5O_7 \cdot 2H_2O$ solution (1 g/100 mL) was added quickly with vigorous stirring. After the color of the mixture changed from pale yellow to wine red, the solution was allowed to reflux for another 15 min. Finally, the Au-NPs colloid acquired was left to cool to room temperature and ultimately stored at 4°C in a refrigerator.

Preparation of the samples. Cabbages and apples were chosen as real samples for the carbendazim detection study. Real sample solutions were prepared according to the previous studies with a slight modification [33]. Simply, 5 g of cabbages and apples was crushed and dissolved in 50 mL of methanol, spiked with 600 ppb carbendazim, and subsequently treated with ultrasonication for 1 h. Insoluble residues were removed via centrifuging at 5000 rpm for 20 min, and cabbage and apple samples were obtained. Finally, real samples with various carbendazim concentrations (Table1) were acquired through dilution.

Detection of carbendazim. Twenty mL of the Au-NPs colloid was diluted in 20 mL tri-distilled water, and 40 mL of the Au-NPs colloid utilized as the stock liquid was acquired for the detection of carbendazim. Upon detection, 1 mL samples (control, carbendazim, interferences, and real sample) were incubated with 2 mL of the Au-NPs colloid under optimal conditions. Color changes were recorded using a digital camera, and absorbance spectra changes were qualitatively and quantitatively monitored on a UV-vis spectrophotometer.

Instruments and measurements. The morphology of newly synthesized Au-NPs was characterized by transmission electron microscopy (TEM) (Zeiss Libra200, Carl Zeiss Jena, Germany). UV-vis absorption spectra were achieved on a Lamda-900 UV-VIS spectrophotometer (Perkin-Elmer). A digital camera (Sony DSC-F717) was utilized to acquire digital photos.

Results and discussion. *Characterization of the Au-NPs.* As shown in Fig. 1a, the UV-vis spectrum of the Au-NPs was dominated by a single, intense peak at 520 nm, which suggested that the prepared Au-NPs were in good monodispersity due to the electrostatic repulsion between them. In order to probe into the morphology and dispersity of the Au-NPs, TEM measurements were carried out. Figure 1b shows the representative TEM image of the Au-NPs, which confirmed that the resultant nanoparticles displayed good monodispersity and a uniform size. These experimental phenomena were consistent with the reported findings on the characterization of Au-NPs [29].

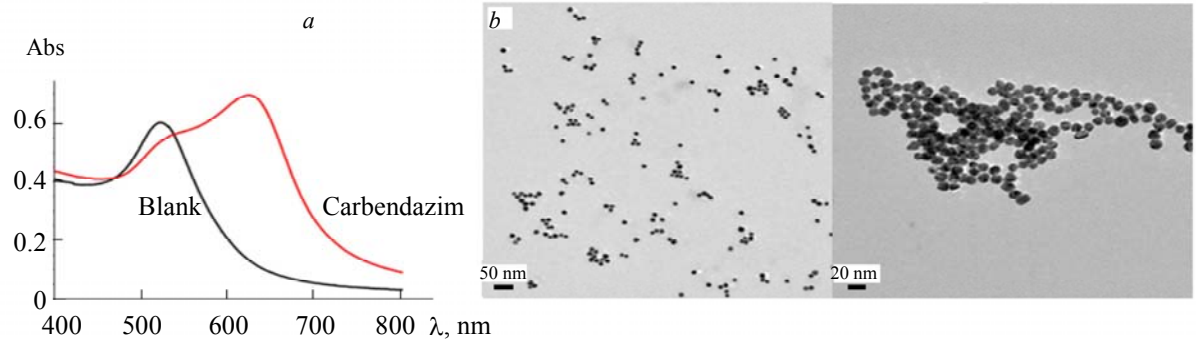

Fig. 1. UV-vis spectrum (a) and TEM images of Au-NPs before and after incubation with carbendazim for 20 min (b).

Colorimetric detection of carbendazim. Electron-rich nitrogen bind to the surface of Au-NPs via Au-N bonds. Accordingly, the average distance between the Au-NPs decreased, which resulted in the aggregation of the Au-NPs accompanied by a color change from red to blue [27]. Upon addition of carbendazim, the color of the Au-NPs colloid changed from red to blue. Figure 2a shows that the absorbance of the Au-NPs colloid rose at 624 nm and decreased at 520 nm. This suggests that the Au-NPs were aggregated after the addition of carbendazim [27, 34]. To test the difference in the morphology of the Au-NPs before and after incubation with carbendazim, TEM was performed. As is shown in Fig. 2b, the absolute Au-NPs colloid exhibits great monodispersity. On the other hand, after incubation with carbendazim for about 20 min, Au-NPs were accumulated, which led to the color change of the Au-NPs. Thus, carbendazim can be easily detected by the Au-NPs-based colorimetric method and quantitatively monitored using a UV-vis spectrophotometer.

Optimization of the detection condition. To optimize the conditions for the carbendazim assay, various factors, including the incubation time, concentration of Au-NPs, incubation temperature, and pH reaction were investigated. All the experiments were operated at room temperature in the absence and presence of carbendazim having a concentration of 600 ppb.

The incubation time plays the dominant role in the reaction. Herein, the reaction time was investigated first. The effect of the incubation time varying from 1 to 30 min on the UV-vis spectrum of the Au-NPs was examined. After the addition of carbendazim, the ratio $R = A_{624}/A_{520}$ increased gradually. As depicted in

Fig. 2a, the *R* value almost reached equilibrium after 20 min, which meant that the reaction almost reached saturation. Thus, 20 min was selected as the optimal incubation time for further study.

The concentration of Au-NPs also exerts an important impact on the trace analysis based on Au-NPs. As shown in Fig. 2a, upon addition of carbendazim, the concentration of Au-NPs, varying from 3.4 to 9.4 nM, was studied. The value of *R* increased gradually with increase in Au-NPs concentration. It reached its maximum at a concentration of 6 nM. Subsequently, a slight and gradual decrease in the *R* value was observed when the Au-NPs concentration exceeded 6 nM. Furthermore, the Au-NPs tended to reaggregate at a higher concentration, as shown by the black broken line in the absence of carbendazim. Hence, the Au-NPs concentration of 6 nM was chosen as optimal for the subsequent research.

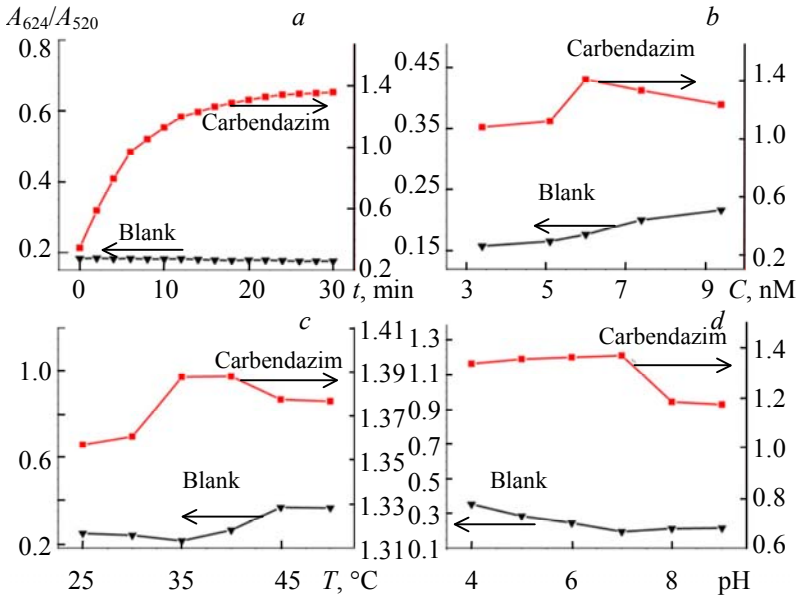

Fig. 2. The plots of the ratio A_{624}/A_{520} of Au-NPs in the absence and presence of 600 ppb carbendazim in different (a) incubation time, (b) concentrations of Au-NPs, and (c) reaction temperature, and (d) the pH.

The incubation temperature ranging from 25 to 50ºC was also investigated. On the one hand, as can be seen from Fig. 2b, before the addition of carbendazim a change in *R* was observed when the incubation temperature was lower than 40ºC, and *R* increased when the incubation temperature exceeded 40ºC. On the other hand, upon addition of carbendazim, the *R* value attained its maximum within the temperature range 35–40ºC. Therefore, the incubation temperature of 35ºC was chosen as optimal for carbendazim detection.

Also we studied the effect of varying the pH from 4 to 9 on the Au-NPs colloid. As one can see from Fig. 2d, when the pH was less than or equal to 7, the *R* value decreased slightly in the absence of carbendazim, while it was almost unchanged in the presence of carbendazim. This means that in a weak acid medium Au-NPs tend to aggregate, which can be caused by a slightly broken electrostatic equilibrium between them because of the presence of positively charged H^+ ions. Nevertheless, the *R* value decreased sharply upon addition of carbendazim when the pH exceeded 7. This is a result of the impact of the negatively charged OH^- ions. Thus, it is clear that the pH of 7 can be chosen as the optimal condition.

Sensitivity of carbendazim. In order to investigate the sensitivity of the sensor system, 1 mL of carbendazim with a concentration (ranging from 0 to 1000 ppb) was added into the Au-NPs colloid (2 mL) under optimal detection conditions. The color of the colloid changed from wine red to blue if the carbendazim concentration increased. The results were further demonstrated by the UV-visible spectrum. As shown in Fig. 3a, the absorption peak broadened at 520 nm and increased in the range from 600 to 650 nm gradually. In addition, as depicted in Fig. 3b, the Au-NPs show a remarkable linear relationship (R^2 = 0.99) with the carbendazim concentration varying from 10 to 600 ppb with a detection limit up to 3.4 ppb (LOD = 3σ/*S*). These results confirmed that the sensor system based on Au-NPs displayed satisfactory sensitivity towards carbendazim at low concentrations.

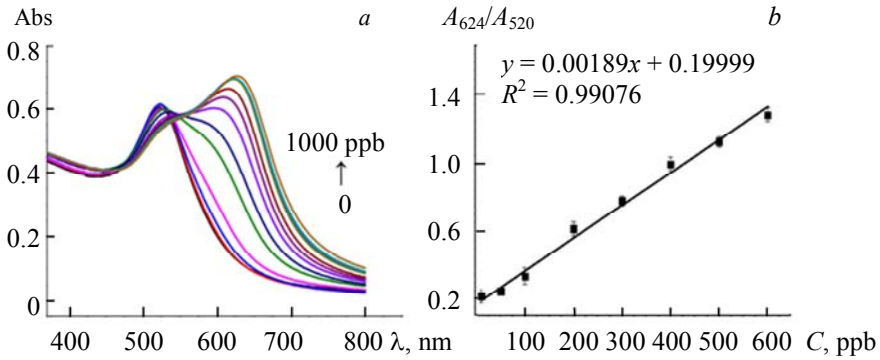

Fig. 3. UV-vis spectra of Au-NPs upon incubation with carbendazim in various concentration ranging from 0 to 1000 ppb under optimal detection conditions (a) and plots of the absorption ratio (A_{624}/A_{520}) vs the carbendazim concentration ranging from 10 to 600 ppb (b).

Interference study. The selectivity of the sensor system was be tested. Different compounds (trichlorfon, lindane, aminotriazole, trietazin, deltamethrin, triazolone, chlorpyrifos, and marathion), which are among the most common insecticides, were detected by the colorimetric method to demonstrate its selectivity. We can evaluate it with the naked eye and quantitatively estimate the *R* value. The results are shown in Fig. 4. The color of the Au-NPs colloid showed no obvious change after incubation with other pesticides, while the Au-NPs colloid changed from red to blue upon addition of carbendazim. The *R* value for carbendazim was nearly 5 times higher than that for the others even at lower concentrations. The results indicate that most insecticides can not disturb the selective detection of carbendazim by this method. This can be attributed to the interaction between carbendazim and Au-NPs, which is much stronger.

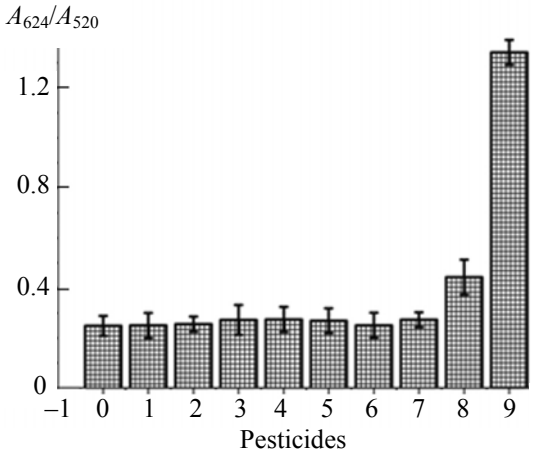

Fig. 4. Plot of A_{624}/A_{520} vs. samples tri-distilled water (0), trichlorfon (1), lindane (2), aminotriazole (3), trietazin (4), deltamethrin (5), triazolone (6), chlorpyrifos (7), marathion (8), and carbendazim (9).

Analysis of carbendazim in spiked real samples. To validate the reliability of the method, it was used to detect carbendazim in cabbages and apples. The real samples spiked with carbendazim of 100, 300, and 600 ppb, respectively, were obtained according to standard methods. The results obtained in the standard addition method are listed in Table 1. As displayed in Table 1, excellent recoveries varying from 87.37 to 104.49% with an average value of 99.13% were obtained in satisfactory repeatability. As compared with some other reported methods [16, 21, 35], the novel method developed in this work showed several advantages, especially in the detection time and convenience when used for the determination of carbendazim in real samples. The results indicated that the colorimetric sensor based on Au-NPs presented here displayed a great potential for real application in carbendazim analysis.

TABLE 1. Application of the Proposed Method for the Determination of Carbendazim in Cabbages and Apples Spiked with Different Amounts of Carbendazim

Samples	Carbendazim concentration, ppb	Measured concentration, ppb (n = 3)	Recovery, % (n = 3)
Cabbage 1	100	99.5±1.598	99.50
Cabbage 2	300	262.13±6.918	87.37
Cabbage 3	600	626.96±2.229	104.49
Apple 1	100	96.02±7.919	96.02
Apple 2	300	321.77±7.758	110.10
Apple 3	600	583.60±6.284	97.27

Conclusion. We have developed a simple, rapid, and effective colorimetric sensor based on Au-NPs for the determination of carbendazim. Au-NPs serve as a colorimetric receptor in the sensor. Carbendazim can be monitored by the color change of the solution verified by the ratio of absorption coefficients via a UV-vis spectrometer without using any advanced instruments. The results suggested that Au-NPs showed good selectivity with a wide linear range from 10 to 600 ppb and a detection limit of 3.4 ppb. Real sample analysis also showed good nondisturbance with satisfactory recovery. This demonstrates that Au-NPs can be a promising tool for fast carbendazim analysis.

Acknowledgment. This work was supported by the National Natural Science Foundation of China (No. 31171684), the Key Technologies R&D Program of China (2014BA07B02), the Chongqing Graduate Student Research Innovation project, China (No. CYB15026), and the Liquor Making Biology, Technology and Application of the Key Laboratory Program of Sichuan Province, China (No. NJ2014-03).

REFERENCES

1. M. Chen, Z. Zhao, X. Lan, Y. Chen, L. Zhang, R. Ji, L. Wang, *Measurement.*, **73**, 313–317 (2015).
2. X. Deng, X. Chen, K. Lin, G. Ding, P. Yao, *Food Anal Method.*, **6**, 1576–1582 (2013).
3. X.-Y. Dong, B.-J. Qiu, X.-W. Yang, D. Jiang, K. Wang, *Electrochemistry*, **82**, 1061–1066 (2014).
4. N. G. Khare, R. A. Dar, A. K. Srivastava, *Electroanalysis*, **27**, 1915–1924 (2015).
5. Z.-Q. Kong, F.-S. Dong, X.-G. Liu, J. Xu, Y. Gong, W.-L. Shan, Y.-Q. Zheng, *Chinese J. Anal. Chem.*, **40**, 474–477 (2012).
6. E. J. Llorent-Martinez, J. Alcantara-Duran, A. Ruiz-Medina, P. Ortega-Barrales, *Food Anal. Method*, **6**, 1278–1283 (2013).
7. C. Lesueur, M. Gartner, A. Mentler, M. Fuerhacker, *Talanta*, **75**, 284–293 (2008).
8. M. Hiemstra, A. de Kok, *J. Chromatogr. A*, **1154**, 3–25 (2007).
9. M. Radisic, S. Grujic, T. Vasiljevic, M. Lausevic, *Food Chem.*, **113**, 712–719 (2009).
10. N. Campillo, P. Vinas, G. Ferez-Melgarejo, M. Hernandez-Cordoba, *J. Agric. Food Chem.*, **61**, 4799–4805 (2013).
11. O. Esturk, Y. Yakar, Z. Ayhan, *J. Food Sci. Technol.*, **51**, 458–466 (2014).
12. A. Lopez Monzon, D. Vega Moreno, M. E. Torres Padron, Z. Sosa Ferrera, J. J. Santana Rodriguez, *Anal. Bioanal. Chem.*, **387**, 1957–1963 (2007).
13. Q. Wu, Y. Li, C. Wang, Z. Liu, X. Zang, X. Zhou, Z. Wang, *Anal. Chim. Acta*, **638**, 139–145 (2009).
14. O. Zamora, E. E. Paniagua, C. Cacho, L. E. Vera-Avila, C. Perez-Conde, *Anal. Bioanal. Chem.*, **393**, 1745–1753 (2009).
15. Z.-F. Chen, G.-G. Ying, H.-J. Lai, F. Chen, H.-C. Su, Y.-S. Liu, F.-Q. Peng, J.-L. Zhao, *Anal. Bioanal. Chem.*, **404**, 3175–3188 (2012).
16. B. Phansawan, T. Prapamontol, P. Thavornyutikarn, S. Chantara, A. Mangklabruks, C. Santasup, *Chiang Mai J. Sci.*, **42**, 681–690 (2015).
17. S. Takeda, K. Fukushi, K. Chayama, Y. Nakayama, Y. Tanaka, S. Wakida, *J. Chromatogr. A*, **1051**, 297–301 (2004).
18. S. Luo, Y. Wu, H. Gou, *Ionics*, **19**, 673–680 (2013).
19. P. Noyrod, O. Chailapakul, W. Wonsawat, S. Chuanuwatanakul, *J. Electroanal. Chem.*, **719**, 54–59 (2014).

20. C. A. Razzino, L. F. Sgobbi, T. C. Canevari, J. Cancino, S. A. S. Machado, *Food Chem.*, **170**, 360–365 (2015).
21. Y. Ya, T. Wang, L. Xie, J. Zhu, L. Tang, D. Ning, F. Yan, *Anal. Method.*, **7**, 1493–1498 (2015).
22. J. Sun, L. Guo, Y. Bao, J. Xie, *Biosens. Bioelectron.*, **28**, 152–157 (2011).
23. D. Zhu, X. Li, X. Liu, J. Wang, Z. Wang, *Biosens. Bioelectron.*, **31**, 505–509 (2012).
24. B. Imene, Z. Cui, X. Zhang, B. Gan, Y. Yin, Y. Tian, H. Deng, H. Li, *Sensor. Actuator B: Chem*., **199**, 161–167 (2014).
25. X. Zhang, Z. Sun, Z. Cui, H. Li, *Sensor. Actuator B: Chem.,* **191**, 313–319 (2014).
26. D. Liu, W. Chen, J. Wei, X. Li, Z. Wang, X. Jiang, *Anal. Chem.*, **84**, 4185–4191 (2012).
27. W. Liu, D. Zhang, Y. Tang, Y. Wang, F. Yan, Z. Li, J. Wang, H. S. Zhou, *Talanta*, **101**, 382–387 (2012).
28. A. D. Strickland, C. A. Batt, *Anal. Chem.*, **81**, 2895–2903 (2009).
29. S. Morais, O. Tavares, P. C. Baptista-Paiga, C. Delerue-Matos, *Anal. Lett.*, **37**, 3271–3286 (2004).
30. L. N. Furini, C. J. L. Constantino, S. Sanchez-Cortes, J. C. Otero, I. Lopez-Tocon, *J. Colloid Interface Sci.*, **465**, 183–189 (2016).
31. N. T. K. T. Wolfgang Haiss, Jenny Aveyard, David G. Fernig, *Anal. Chem.*, **42**, 4103–4110 (2007).
32. X. S. Xiaohui Ji, Jun Li, Yubai Bai, Wensheng Yang, Xiaogang Peng, *J. Am. Chem. Soc.,* **53**, 2438–2443 (2007).
33. J. Sun, L. Guo, Y. Bao, J. Xie, *Biosens. Bioelectron.*, **28**, 152–157 (2011).
34. Z. Sun, Z. Cui, H. Li, *Sensor. Actuator B: Chem.,* **183**, 297–302 (2013).
35. H. Yan, L. Liu, N. Xu, H. Kuang, C. Xu, *Food. Agr. Immunol.*, **26**, 659–670 (2015).